HiViS: Hiding Visual Tokens from the Drafter for Speculative Decoding in Vision-Language Models

Zhinan Xie[1,2] Peisong Wang[1,2,3] Jian Cheng[1,2,3,4]
[1]C[2]DL, Institute of Automation, Chinese Academy of Sciences
[2]School of Artificial Intelligence, University of Chinese Academy of Sciences
[3]AIRIA [4]Maicro.ai
xiezhinan2025@ia.ac.cn, {peisong.wang, jcheng}@nlpr.ia.ac.cn

Abstract

*Speculative decoding is an effective approach for accelerating inference in Large Language models (LLMs), but its adaptation to Vision-Language models (VLMs) remains challenging for additional visual tokens in multimodal inputs. First, owing to the fact that the drafter and the target VLM may derived from different families, the semantic representations of visual tokens in the target VLM are misaligned with those in the drafter, introducing bias into the KV-cache during the prefill stage. Second, the large number of visual tokens substantially slows down the drafter's self-attention during the decoding stage. We propose **H**iding **V**isual Tokens from the Drafter for **S**peculative Decoding in Vision-Language Models (**HiViS**), an explicit-implicit input decomposition framework that alleviates the above inefficiency. All visual tokens are removed from the drafter's input, retaining only textual tokens as explicit inputs, while directly reusing the target VLM's corresponding last-layer hidden states as implicit visual information without additional processing. To train the drafter efficiently, we introduces multi-step self-feedback training strategy with dynamic data selection and sequential embedding supervision to simulate reasoning during training. Our approach compresses the prefill sequence length of the drafter to only $0.7\% - 1.3\%$ of the target VLM's input, while maintaining lossless generation quality. Extensive experiments across diverse models and tasks demonstrate up to $2.65\times$ speedup, confirming the effectiveness of HiViS in accelerating VLM inference.*

1. Introduction

Autoregressive (AR) models, including Large Language models (LLMs) [1, 3, 7] and Vision–Language models (VLMs) that incorporate LLM [1, 14, 18, 19, 25], achieve strong generative performance but suffer from severe latency due to strictly sequential inference. Speculative decoding [5, 13, 28] addresses this limitation by introducing a lightweight drafter that proposes candidate tokens and a target model that verifies them in parallel, thereby reducing decoding steps while preserving fidelity. While extensively investigated in LLMs [4, 8, 9, 15, 23], its application to VLMs remains under-explored.

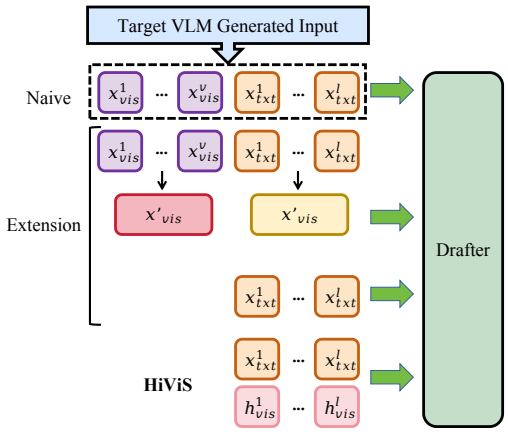

Figure 1. Comparison of speculative decoding input modality for VLM drafters. The naive method directly reuses both visual and textual tokens from the target VLM. Extensions either process visual and textual tokens differently or remove visual tokens without other visual information. HiViS hides all visual tokens, retaining only text tokens as explicit input and augmenting them with implicit visual semantics.

Naively extending speculative decoding from LLMs to VLMs, as illustrated in Fig. 1, faces several fundamental obstacles: **(1) Visual Semantic Gap.** Visual tokens produced by the target VLM's encoder are tailored to its own representational space and misaligned with that of a lightweight drafter, introducing semantic inconsistency and bias in the KV-cache during prefill. This mismatch amplifies distributional discrepancy during drafting and reduces the accep-

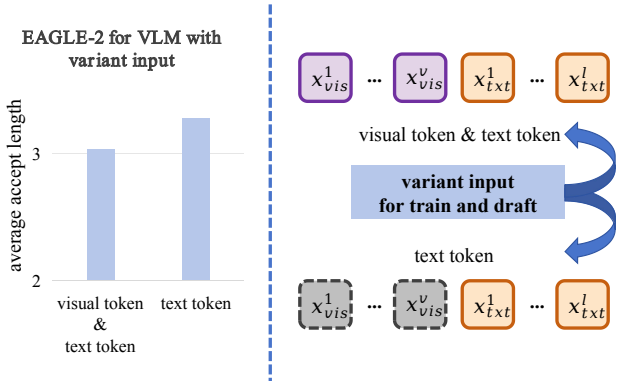

Figure 2. EAGLE-2 [16] trained on the same multimodal dataset under two settings: full visual–text inputs versus text-only inputs with all visual tokens deleted, evaluated on LLaVA-Next 7B with ChartQA at temperature 0.

tance rate. To validate this, we adapted EAGLE-2 [16], a remarkable speculative decoding framework for LLM, to a multimodal setting and trained it under two configurations: one with both text tokens and target VLM-generated visual tokens, and one with only text tokens. As shown in Figure 2, the text-only configuration achieved better performance, confirming that directly reusing visual tokens can impede rather than facilitate speculative decoding. **(2) Computational Burden of Long Visual Token Sequences.** Although the drafter remains lightweight to ensure efficiency, the requirement to handle long and complex visual token sequences increases its computational overhead. For instance, LLaVA-NeXT [19] produces over 2,000 visual tokens when processing high-resolution images, making visual inputs the dominant factor in sequence length and severely slowing down the drafter.

Current approaches for speculative decoding in VLMs inadequately address the challenges of visual tokens. As shown in Figure. 1, some methods constrain the drafter to text-only inputs [10], discarding visual semantics altogether. Others, such as MSD [17], decouple text and visual channels but still oblige the drafter to process both, retaining the inefficiency of long visual sequences. IbED [12] apply diverse processing strategies to visual tokens and fuse them with textual representations through ensemble drafting, yet this further amplifies alignment complexity. Consequently, the semantic gap and computational burden introduced by visual tokens remain unresolved.

In this work, we propose **H**iding **V**isual Tokens from the Drafter for **S**peculative Decoding in Vision–Language Models (**HiViS**), a speculative decoding framework for VLMs that removes all visual tokens from the drafter yet still remaining visual information. We design an explicit-implicit input scheme, where text tokens serve as explicit inputs. Given that textual hidden states in the target VLM are enriched with visual information through cross-attention, we exploit the target VLM to provide implicit visual inputs, thereby reducing semantic misalignment between the two models. While this scheme constructs a compact and semantically consistent KV-cache that accelerates decoding, the drafter cannot directly access updated visual semantics during independent drafting. To address this, we introduce a dynamic self-regulated multi-step training strategy that simulates inference with sequential supervision and dynamically filters within-capacity yet challenging samples, thereby enabling the drafter to autonomously propagate and update visual semantics.

In conclusion, our contributions are as follows:

- An explicit–implicit input design for lossless VLM speculative decoding, where all visual tokens are removed and the drafter relies solely on text tokens and implicit visual guidance without extra alignment operation, yielding a compact and accurate KV-cache that accelerates decoding under a lightweight architecture.
- A dynamic self-regulated multi-step training strategy with a data filtering mechanism that prioritizes effective examples and enabling the model to autonomously propagate and update visual semantics for independent stable drafting.
- Comprehensive empirical validation. Experiments across representative multimodal tasks consistently demonstrate the effectiveness of HiViS, showing significant improvements in acceptance rate and speedup ratio while preserving the output distribution of the target model.

2. Preliminaries

2.1. Speculative Decoding

Speculative decoding has emerged as a promising technique to accelerate inference in LLMs by leveraging a lightweight drafter M_q to generate multiple candidate tokens for the following γ timesteps, which are then verified in parallel by the target LLM M_p. During the verification process, the decoding identifies the prefix of candidate tokens preceding the first one rejected by speculative sampling, the target LLM then uses an adjusted distribution to resample a next token, which is appended to the sequence. If all candidate tokens are accepted, the target LLM samples a new token based on its original distribution and appends it to the end of the sequence. Let n denote the total number of tokens produced by the target LLM during this decoding step, representing the effective inference length in this round. This approach reduces sequential decoding steps, enabling the target LLM to generate multiple tokens per forward pass and improving inference efficiency without sacrificing output quality.

Previous studies[5, 13] have shown that the effectiveness of speculative decoding is closely tied to the value of n, the number of candidate tokens generated by the drafter in each

iteration. The optimal choice of n depends on two key factors: the inference speed of the drafter and the alignment quality between the draft and target models. A drafter that is both faster and better aligned with the target LLM can support a larger n, thereby improving the acceptance rate of candidate tokens and yielding greater speedups in speculative decoding.

2.2. Large VLMs

Modern VLMs hat incorporate LLM have evolved from training multimodal encoders from scratch to adopting pretrained large language models (LLMs) as the backbone, aligning visual features with powerful text generation capabilities. Architecturally, VLMs typically comprise three key components: a vision encoder that projects image or video data into high-level embeddings, a projector that maps these embeddings into the textual embedding space, yielding v visual embeddings of dimension d, denoted as $e_{visual} \in \mathbb{R}^{v \times d}$, and an LLM decoder that autoregressively generates text. At each decoding step, the LLM conditions not only on the v visual embeddings but also on the l textual embeddings from the input sequence x_{text}, $e_{text} \in \mathbb{R}^{l \times d}$, together with all previously generated tokens. Formally, the model iteratively samples the next token x_{new} from the distribution $p(\cdot \mid e_{visual}, e_{text}, e_{gen})$, where e_{gen} denotes the set of embeddings of the tokens generated in earlier decoding steps. This structure enables the reuse of robust LLM architectures such as Emu3 [27] with LLaMA [25], LLaVA [18] with Vicuna [6], and QWen2-VL [26] with QWen2 [24], while integrating visual information via projection layers or cross-attention mechanisms.

When using LLMs as backbones, two common training strategies are employed. Joint training updates the parameters of the LLM, projector, and vision encoder simultaneously, enabling strong cross-modal fusion but often at high computational cost. In contrast, freeze-based training selectively freezes parts of the model—most often the LLM—to preserve its pre-trained linguistic knowledge, while updating projector or vision encoder layers to adapt to multimodal alignment. This trade-off allows models such as Flamingo [2] and LLaVA [18] to achieve effective vision-language grounding without sacrificing the language generation capability inherited from large-scale LLM pretraining. In summary, these designs underscore the central role of LLM backbones in scaling VLMs, where vision encoders provide robust visual representations and LLMs function as the primary components for reasoning and text generation.

3. Methodology

Existing approaches to speculative decoding in VLMs inadequately handle visual tokens: whether directly feeding them into the drafter or applying additional processing, both introduce extra computation and incur additional decoding overhead, while also risking semantic misalignment with the target VLM. Our key insight is that visual semantics can be preserved without directly processing visual tokens by leveraging cross-attention–enriched textual hidden states from the target VLM. Building on this observation, we propose an explicit–implicit input scheme that hides all visual tokens from the drafter's input, retains only **explicit text tokens**. Inspired by the representation guidance in EAGLE-2 [16], we augment input of the one-layer-decoder drafter with the textual last hidden state from the target VLM as visual guidance, thereby constructing a compact and semantically consistent KV-cache that accelerates decoding.

To enable the drafter to autonomously propagate and update visual information during independent inference where direct guidance from the target VLM is unavailable, we design a dynamic self-regulated multi-step training strategy inspired by the harmonized representation principle in HASS [30], and simulates the drafter's independent inference process. Specifically, we introduce a step-dependent **dynamic sequential embeddings** that are concatenated to the inputs at each decoding step, thereby providing auxiliary supervision to guide the drafter's inference process. These sequential embeddings are jointly optimized within a multi-step self-feedback training paradigm, where the drafter is supervised to simulate its own inference process. This adaptation ensures that both the drafter parameters and the sequential embeddings are tuned for drafting, enabling the drafter to autonomously generate implicit inputs that carry latest visual semantics without latest guidance from the target model. Furthermore, we introduce a dynamic data filtering mechanism that discards examples where the drafter consistently fails, and focuses training on instances that are within the drafter's capacity but not yet well mastered, leading to more efficient use of data.

In summary, our one-layer-decoder drafter operates on inputs with three components: explicit textual tokens to provide linguistic content, implicit visual guidance from the target VLM to supply visual semantics without explicit tokens, and dynamic sequential embeddings to regulate and supervise the drafting process across multiple steps.

3.1. Explicit-Implicit Input Reformulation and Drafter Workflow

As illustrated in Figure. 3, the input to the target VLM M_p consists of two modalities: visual tokens and text tokens. The visual branch is obtained by passing the image through a vision encoder followed by a multimodal projector, producing a sequence of v visual embeddings $e^1_{visual}, \ldots, e^v_{visual}$. In parallel, the text branch is formed by embedding the input tokens, yielding $e^1_{text}, \ldots, e^l_{text}$. Within the target VLM M_p, cross-attention between textual and visual tokens ensures that the hidden states at text positions are enriched with visual information. The last-layer

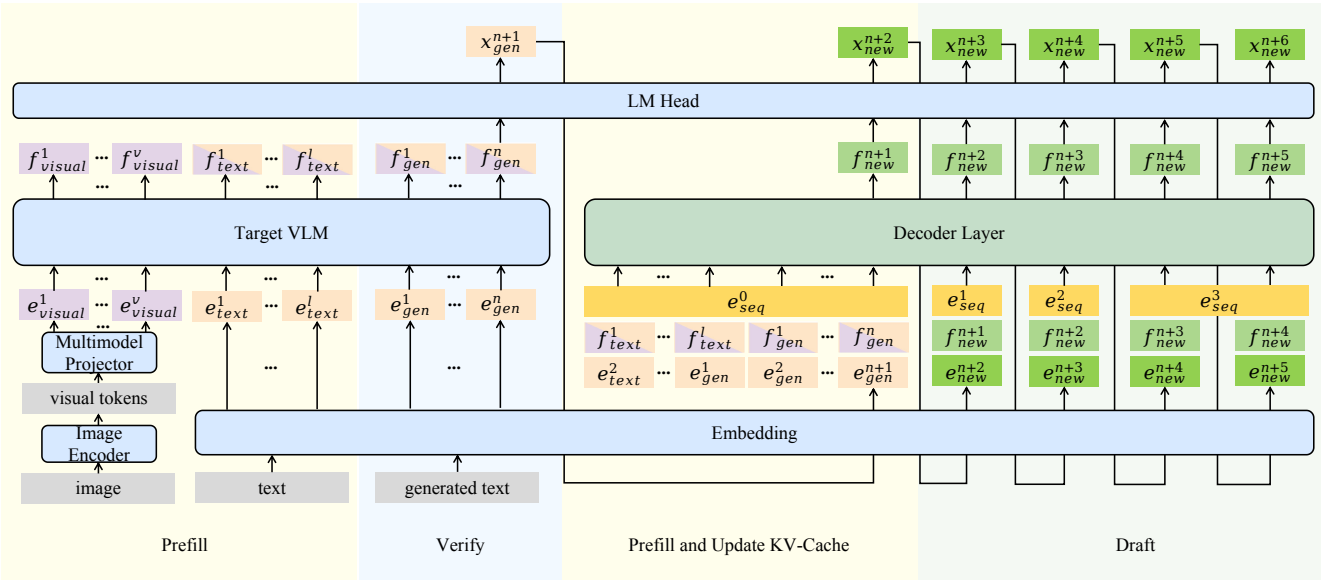

Figure 3. Overview of HiViS. The target VLM first performs Prefill, where image inputs are encoded by a vision encoder and projected into visual embeddings e_{visual}, and text tokens are embedded to e_{text}. During Verify, the target VLM produces both token embeddings e_text and their last-layer hidden states f_{text} in parallel. The Drafter Prefill and KV-cache Update stage initializes the drafter with e_text and f_{text}, and a sequential embedding e^0_{seq}, while accepted outputs f_{gen} and e_{gen} from the verify stage are appended to the cache. Finally, in the Draft stage, the lightweight drafter autoregressively generates candidate tokens x_{new}, dynamically concatenating step-dependent e_{seq} to stabilize multi-step generation.

hidden state at position t is given by:

$$f^t_{text} = M_p(e^1_{visual}, \ldots, e^v_{visual}, e^1_{text}, \ldots, e^{t-1}_{text}) \quad (1)$$

During inference, our framework operates in four coordinated stages.

Prefill of the Target VLM: The target VLM first consumes the complete multimodal prefix, which includes both visual embeddings derived from the image encoder and projector, and textual embeddings obtained from the textual input tokens. Through cross-attention, the model computes last hidden states in which the textual representations are enriched with visual information. This step establishes the initial multimodal representation.

Verification by the Target VLM: The target VLM then performs verification in a batched manner. Instead of producing tokens strictly one by one, it evaluates every candidate segment proposed by the drafter within a single forward pass. For each position in this segment, the target model produces the corresponding token distribution, yielding the associated last-layer hidden states f_{gen} of the generated embeddings e_{gen}. These outputs provide ground-truth multimodal context that determines which of the drafter's predictions are accepted and which are rejected. In Fig. 3, the embeddings denoted as e_{gen} correspond to the accepted segment, which is committed to the output sequence and subsequently used to update the drafter's KV-cache.

Drafter Prefill and Cache Update: Before entering its own drafting stage, the lightweight drafter performs a prefill step. At this point, its inputs consist solely of the textual embeddings e^{t+1}_{text} as explicit text information, concatenated with the corresponding last-layer hidden states f^t_{text} provided by the target model as implicit visual information, and the initial sequential embedding, denoted as e^0_{seq}. This combination initializes the drafter's KV-cache with both textual and implicit visual information.

After verification, the drafter updates its cache by appending the newly generated embeddings e_{gen} together with their hidden states f_{gen}, again augmented with the e^0_{seq}. The latest KV-cache can be expressed as:

$$\text{KV Cache} = \Big(Linear_{key}(InputState), Linear_{value}(InputState)\Big), \quad (2)$$

where the $InputState$ is:

$$InputState = \Big[e^2_{text} \| f^1_{text} \| e^0_{seq}, \cdots, e^l_{text} \| f^{l-1}_{text} \| e^0_{seq}, e^1_{gen} \| f^l_{text} \| e^0_{seq}, \cdots, e^{n+1}_{gen} \| f^n_{gen} \| e^0_{seq}\Big]. \quad (3)$$

$\|$ represents the concatenate operation. This ensures that all visual grounding is inherited indirectly while keeping the cache length minimal.

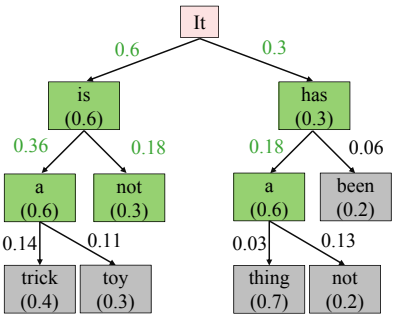

Figure 4. An illustration of token-tree construction during inference, where nodes represent candidate tokens with associated probabilities and path scores.

Drafting with the Lightweight Model: Once the KV-cache has been initialized, the drafter enters the drafting phase, where it autoregressively generates candidate tokens. At each decoding step, the input is dynamically augmented with a step-dependent sequential embedding, ensuring that different time steps are explicitly distinguished in the self-attention context. Formally, given the existing KV-cache and previously generated pairs of token embeddings and hidden states, the hidden state at step $n + t (t > 1)$ is computed as

$$f_{new}^{n+t} = M_q(\text{KV Cache}, e_{new}^{n+2} \| f_{new}^{n+1} \| e_{seq}^{1}, \cdots, e_{new}^{n+s} \| f_{new}^{n+s-1} \| e_{seq}^{i}, \cdots, e_{new}^{n+t} \| f_{new}^{n+t-1} \| e_{seq}^{i}) \quad (4)$$

where e_{seq}^{i} denotes the sequential embedding associated with time position s, with the index defined as $i = \min(s, \text{threshold})$. The threshold is a hyperparameter, set to 3 in our experiments, in order to reduce training burden.

This formulation ensures that the drafter not only conditions on text history and implicit visual information but also maintains explicit temporal alignment across multiple steps. By dynamically inputting sequential embeddings, the drafter stabilizes long generation and mitigates degradation, leading to more reliable speculative predictions.

During token generation, we adopt the token-tree construction strategy of EAGLE-2[16], as illustrated in Figure. 4. We builds a token tree with fixed depth, where each node represents a candidate token and is scored by the cumulative product of token probabilities along its path from the root, reflecting the confidence of that generation path. At each level, every node expands into its top-k predictions, yielding up to k^2 candidates. These are then ranked by their path scores, and the top-k nodes are retained as parents for the next layer. After reaching the fixed depth, the n highest-scoring paths are selected, and their terminal tokens are used as candidate outputs of the drafter. In our figure, n is set to 5.

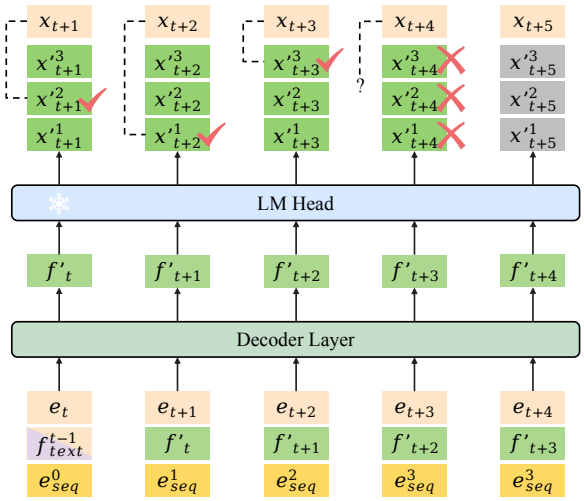

Figure 5. Training architecture of HiViS. e_{t+n} are input embeddings, f_{t-1} and x_{t+n} are hidden states and tokens from the target VLM, while f'_{t+n} and x'^{k}_{t+n} are outputs from the drafter. Correct predictions are marked with ✓, errors with ×, and gray tokens denote discarded candidates.

3.2. Dynamic training

We have two training objectives: (i) to align the drafter's token predictions with those of the target VLM, ensuring alignment in output distribution. (ii) To align the drafter's hidden states with the corresponding last-layer hidden states of the target VLM, thereby enabling the drafter to learn the progressive update of visual semantics that occurs during inference.

Our training objective is to align the drafter's representations with the corresponding last-layer hidden states of the target VLM, thereby enabling the drafter to learn the progressive update of visual semantics that occurs during inference.

training framework: As shown in Figure 5, to improve training efficiency and reduce memory consumption, we employ fixed embedding vectors of the dataset sequence $[e_1, e_2, \cdots]$ as inputs during training. Meanwhile, for each time step, we precompute the corresponding target hidden states $[f_{text}^{1}, f_{text}^{2}, \cdots]$ and the greedily predicted token sequence $[x_2, x_3, \cdots]$ using the target VLM. For example, the hidden state f_t denotes the representation produced by the target VLM M_p at step t given the sequence up to step t, i.e., $f_t = M_p(e_1, \cdots, e_t)$. Similarly, x_{t+1} is the token obtained by greedy decoding from the LM head applied to the last-layer hidden state, which is $x_{t+1} = \arg\max(\text{LM head}(f_t))$.

Following the setup in Figure 5, during training we assume that the inference begins at step t. The first forward pass of the drafter M_q starts from the hidden state generated by the target VLM and concatenates the corresponding

embedding vectors to form its input, producing a predicted hidden state:

$$f'_t = M_q\big(e_2 \,\|\, f^1_{text} \,\|\, e^0_{seq},\ \cdots,\ e_t \,\|\, f^{t-1}_{text} \,\|\, e^0_{seq}\big)\,. \quad (5)$$

Subsequently, the n-th forward pass ($n > 1$) can be generalized as:

$$\begin{aligned} {f'}_{t+n-1} = M_q(&e_2 \,\|\, f^1_{text} \,\|\, e^0_{seq}, \cdots, e_t \,\|\, f^{t-1}_{text} \,\|\, e^0_{seq}, \\ &e_{t+1} \,\|\, {f'}_t \,\|\, e^i_{seq}, \cdots, e_{t+s-1} \,\|\, {f'}_{t+s-2} \,\|\, e^i_{seq}, \\ &\cdots, e_{t+n-1} \,\|\, {f'}_{t+n-2} \,\|\, e^i_{seq}) \end{aligned} \quad (6)$$

where $i = \min(s-1, \text{threshold})$.

Our training contains two stages, at the stage-1, we only train the drafter with 1 step, and at the stage-2, we train it for $n > 1$ steps. For stage-2, inspired by knowledge distillation [29], the drafter outputs a probability distribution at each step, from which the top-K tokens are selected as candidates. We then apply a dynamic filtering criterion:

$$x_{t+n-1} \in \{{x'}^1_{t+n-1}, \cdots, {x'}^k_{t+n-1}, \cdots, {x'}^K_{t+n-1}\} \quad (7)$$

where ${x'}^k_{t+n-1}$ denotes the token with the k-th highest probability predicted by the drafter. If the target VLM generated ground-truth token x_{t+n-1} falls within the drafter's top-K predictions, the example at step $t+n-1$ is retained for optimization. Otherwise, the simulation for this instance is terminated early and discarded, preventing the model from wasting capacity on consistently mispredicted sequences. For instance, as shown in Figure 5 with $N = 5$, the process stops at the 4_{th} forward pass because the candidate tokens fail to cover the target VLM's prediction, and thus the 5_{th} forward pass is not included in training.

In this way, the stage-1 training establishes a solid foundation for the drafter's predictive capability, while the stage-2 both simulates the token-tree construction process of actual drafting and performs dynamic data filtering. This encourages the drafter to focus on examples within its capacity but insufficiently learned during stage-1, thereby improving training efficiency while fostering its ability to reproduce the progressive update dynamics of visual semantics in target VLM.

Training Loss: In the computation of the training loss, our work follows the formulation adopted in EAGLE [15] and HASS [30]. The overall loss consists of three components, weighted as $L = w_{\text{reg}} L_{\text{reg}} + w_{\text{cls}} L_{\text{cls}} + w_{\text{top-K}} L_{\text{top-K}}$.

- Hidden-state alignment loss: Since the hidden state output f'_t of the drafter at each step will be reused as input for the next forward pass, it is critical to align it with the corresponding last-layer hidden state f_t of the target VLM during training:

$$L_{\text{reg}} = \text{Smooth-}L1(f_t, f'_t). \quad (8)$$

- Probability alignment loss: To encourage the drafter to capture the conditional distribution of the target VLM, we minimize the cross-entropy between the predictive distributions of the two models:

$$L_{\text{cls}} = \text{CrossEntropy}(\text{predict}(f_t), \text{predict}(f'_t)). \quad (9)$$

- Top-K alignment loss: Since speculative decoding requires the drafter to generate a top-K token tree during inference, we further enforce alignment over the high-probability region of the predictive distributions. Let Ω_t denote the set of the top-K tokens predicted by the target model at step t; the loss is defined as

$$L_{\text{top-K}} = -\sum_{x \in \Omega_t} q(x) \log p(x), \quad (10)$$

where $q(x)$ and $p(x)$ denote the probabilities assigned by the target VLM and drafter, respectively.

Mixed Modality Dataset: To ensure that the lightweight drafter can adapt to the explicit-implicit input format, we apply the same preprocessing strategy during training on multimodal datasets. Specifically, instead of storing and feeding full sequences of visual tokens, we retain only the text embeddings together with the corresponding last-layer hidden states from the target VLM, which reduces the storage of the processed dataset by around 90%. As a result, the overall training burden is substantially alleviated while maintaining alignment to multimodal supervision.

Given that the textual components of the multimodal datasets we use are relatively short and have limited vocabulary, while the LLM backbone of target VLM is already highly effective at language generation, we augment our training dataset with an additional text-only dataset by mixing them together. Following prior approaches [10, 17], this augmentation improve the ability to generate fluent and contextually appropriate text for drafter. In this way, the drafter learns "how to speak" while simultaneously learning "how to see."

Since many entries in multimodal datasets contain answers consisting of only a single token, such cases are not useful for multi-step training. We therefore filter the multimodal data by retaining only entries whose answers exceed five words, and apply this filtering in both training stages. For the text-only dataset, no filtering is applied in the stage-1. However, given that programming-related queries are rare in multimodal tasks but occupy a substantial portion of text-only data, we apply an additional filtering step in the stage-2. Specifically, we compute the proportion of programming-related symbols and keywords in each entry, and use this measure to decide whether to retain the sample for training.

Model	Methods	ChartQA		VQAv2		ScienceQA		TextVQA	
		SR	τ	SR	τ	SR	τ	SR	τ
T = 0									
LLaVA-Next 7B	EAGLE-2	1.33x	3.04	1.58x	4.63	1.47x	3.02	1.34x	3.35
	MSD	1.61x	4.38	1.57x	4.86	1.72x	4.08	1.41x	4.00
	HiViS	**1.91x**	**5.20**	**1.81x**	**5.71**	**2.07x**	**4.79**	**1.62x**	**4.57**
LLaVA-Next 13B	EAGLE-2	1.44x	3.21	1.61x	4.62	1.59x	3.02	1.40x	3.35
	MSD	1.75x	4.67	1.64x	4.96	1.95x	4.34	1.53x	4.09
	HiViS	**1.95x**	**5.26**	**1.81x**	**5.71**	**2.22x**	**4.90**	**2.65x**	**4.45**
T = 1									
LLaVA-Next 7B	EAGLE-2	1.10x	2.63	1.39x	3.44	1.25x	2.50	1.18x	2.65
	MSD	1.38x	3.48	1.35x	3.77	1.33x	3.11	1.26x	3.10
	HiViS	**1.65x**	**3.92**	**1.49x**	**4.09**	**1.60x**	**3.32**	**1.34x**	**3.34**
LLaVA-Next 13B	EAGLE-2	1.29x	2.69	1.48x	3.60	1.38x	2.61	1.23x	2.71
	MSD	1.58x	3.64	1.46x	3.91	1.60x	3.23	1.43x	3.24
	HiViS	**1.69x**	**3.79**	**1.55x**	**4.11**	**1.78x**	**3.52**	**1.50x**	**3.50**

Table 1. Speedup ratio (s) and average acceptance length (τ) across benchmarks.

4. Experiment

Models and Tasks: To evaluate the generality and effectiveness of the proposed approach across different task types, we conduct experiments on two representative open-source VLMs: LLaVA-1.5 (7B and 13B) [18] and LLaVA-Next (7B and 13B) [19]. We conduct experiments on common visual question answering benchmarks, including ChartQA [21], VQAv2 [11], ScienceQA[20], and TextVQA [22], all of which assess both image understanding and reasoning capabilities. We evaluate each task on a subset of 80 samples.

Baselines: We compare our method against two baselines. The first is EAGLE-2 [16], which serves as the foundation of our framework. We adapt it to the VLM setting by modifying its inputs to include both visual tokens and text tokens produced by the VLM, and retrain it on the same multimodal dataset as ours. The second is MSD [17], which also applies speculative decoding to VLMs. MSD also leverages both multimodal and text-only datasets for training, but differs in that it directly consumes the full sequence of visual and textual tokens.

Metrics: Since this work adopts speculative decoding as the core mechanism, the experimental evaluation follows the standard protocol in speculative decoding and focuses primarily on improvements in inference latency. To comprehensively assess the efficiency of the proposed method, we employ two commonly used metrics:

- **Speedup Ratio.** This metric measures the acceleration of speculative decoding relative to autoregressive inference with the base model. It is defined as the ratio between the throughput of speculative decoding and that of pure autoregressive generation by the target model. Throughput is measured in tokens per unit time, directly reflecting the practical speedup achievable in deployment.
- **Average Acceptance Length (τ).** This metric denotes the average number of tokens from the drafter that are accepted by the target model in each verification stage. It captures the accuracy of the drafter's multi-step predictions and indicates how closely its outputs align with the target model. A larger average acceptance length implies higher alignment and, consequently, greater efficiency. The value is averaged over all verification steps across the test set to obtain a stable estimate of overall performance.

Together, these two metrics provide complementary perspectives: speedup ratio reflects the gain in inference speed, while average acceptance length characterizes the efficiency of verification.

Training Setup For text-only training data, we use 68,000 dialogue instances from ShareGPT, while for multimodal training we sample 68,000 dialogues from the LLaVA-Mix665k dataset. During training, the maximum draft length is set to $N = 4$, and the number of top candidates for each step is set to $K = 5$. The threshold for the sequantial embedding is set to 3. All other hyperparameters follow EAGLE-2 [16].

Inference Setup: The experiments are conducted on a single A800 GPU with batch size set to 1. In the draft stage, the token tree expands by selecting the top-10 candidates at each layer with a fixed depth of 7, and the top-60 paths ranked by cumulative probability product are retained as candidate outputs.

4.1. Results

Table 1 presents a detailed comparison of speedup ratio and average acceptance length across different VLMs and tasks. Despite excluding any explicit visual information from both training and inference inputs, HiViS consistently outperforms both EAGLE-2 [16] and MSD [17] across all models and tasks. Under temperature 0 with LLaVA-Next-7B, HiViS achieves substantial gains in average acceptance length, exceeding EAGLE-2 by 71% on ChartQA and 59% on ScienceQA,and even surpassing MSD, which consumes full visual inputs, by 19% and 17%, respectively. For the larger LLaVA-Next-13B, HiViS maintains a clear advantage, reaching up to a 2.62× speedup ratio in our hardware environment. At temperature 1, our method continues to maintain advantage, with the average acceptance length ranging from 3.34 to 4.11 and the speedup ratio varying between 1.34× and 1.78×.

Statistical analysis reveals that in TextVQA only 0.7% of the input sequence length is retained on average, while in ChartQA, VQAv2, and ScienceQA the retained proportions are 1.2%, 0.8%, and 1.3%, respectively. Despite employing such a direct truncation strategy that preserves only a very short input sequence, HiViS still achieves high average acceptance lengths and substantial speedup ratios. These results demonstrate that, for VLMs, the drafter in speculative decoding does not require any explicit visual tokens as input, and further validate the effectiveness of our proposed training methodology.

4.2. Ablation Studies

We conduct ablation studies using the LLaVA-Next-7B model on the ChartQA dataset with the temperature fixed at 0. We analyze the effect of training stages and dataset composition on the drafter's performance, as measured by the average acceptance length τ.

training stage	τ
stage-1	4.84
stage-2	5.20

Table 2. The average accept length after stage-1 training and stage-2 training

Effect of multi-stage training. As introduced earlier, our training is divided into two stages. Stage-1 primarily focuses on aligning the drafter with the multimodal and textual input distributions, enabling it to establish a stable foundation for cross-modal reasoning. The training emphasizes robustness and general adaptability, ensuring that the drafter can effectively process both visual and textual tokens. In contrast, Stage-2 is dedicated to aligning the drafter's generated outputs with high-quality target answers through multi-step self-feedback training. This stage further enhances accuracy and consistency, particularly in tasks requiring fine-grained reasoning over multimodal information. Table 2 shows that τ improves from 4.84 in stage-1 to 5.20 in stage-2. This confirms that the second-stage training, which incorporates multi-step self-feedback with top-k guided filtering, enhances the drafter's ability to align with the target VLM over longer drafting.

stage-1 dataset	τ
multimodal dataset only	3.42
text dataset only	4.69
both	4.84

Table 3. The average accept length after the stage-1 training. The training is conducted on three kinds of dataset: multimodal dataset only (LLaVA-Mix665k), text dataset only (ShareGPT), both

Effect of dataset composition. We further investigate the impact of dataset composition in Stage-1 training. Using only the multimodal dataset yields unsatisfactory results, primarily because each multimodal sample is relatively short in length, making it insufficient to independently train the drafter. Training solely on the text dataset achieves comparatively better performance, highlighting the crucial role of abundant textual supervision in strengthening the drafter's reasoning capability. The combination of multimodal and text datasets yields the strongest performance, demonstrating that the two types of data are complementary: multimodal data provides grounding ability while text data enhances reasoning, and their integration leads to the most balanced and effective drafter.

5. Conclusion

We present **H**iding **V**isual Tokens from the Drafter for **S**peculative Decoding in Vision–Language Models (**HiViS**), a speculative decoding framework for VLMs that eliminates explicit visual token consumption while preserving multimodal grounding. By reformulating the drafter's conditioning into explicit textual inputs and implicit hidden-state guidance, DeViS avoids misaligned visual representations in the KV-cache and achieves a compact state representation that accelerates decoding under a lightweight architecture.

To enhance alignment and robustness, we introduce a refined multi-step self-feedback training strategy that integrates dynamic data filtering and step-dependent sequential embeddings. This design enables efficient learning from within-capacity yet challenging examples, maintains stability over long drafting, and equips the drafter with the ability to autonomously propagate and update visual semantics during independent inference.

Comprehensive experiments on LLaVA-Next (7B and 13B) across multiple tasks demonstrate that HiViS consis-

tently surpasses EAGLE-2 and MSD in both speedup ratio and acceptance length, despite retaining only $0.7\% - 1.3\%$ of the input sequence length. These results establish speculative decoding without explicit visual tokens as a viable and effective paradigm for VLMs.

References

[1] Josh Achiam, Steven Adler, Sandhini Agarwal, Lama Ahmad, Ilge Akkaya, Florencia Leoni Aleman, Diogo Almeida, Janko Altenschmidt, Sam Altman, Shyamal Anadkat, et al. Gpt-4 technical report. *arXiv preprint arXiv:2303.08774*, 2023. 1

[2] Jean-Baptiste Alayrac, Jeff Donahue, Pauline Luc, Antoine Miech, Iain Barr, Yana Hasson, Karel Lenc, Arthur Mensch, Katherine Millican, Malcolm Reynolds, et al. Flamingo: a visual language model for few-shot learning. *Advances in neural information processing systems*, 35:23716–23736, 2022. 3

[3] Tom Brown, Benjamin Mann, Nick Ryder, Melanie Subbiah, Jared D Kaplan, Prafulla Dhariwal, Arvind Neelakantan, Pranav Shyam, Girish Sastry, Amanda Askell, et al. Language models are few-shot learners. *Advances in neural information processing systems*, 33:1877–1901, 2020. 1

[4] Tianle Cai, Yuhong Li, Zhengyang Geng, Hongwu Peng, Jason D Lee, Deming Chen, and Tri Dao. Medusa: Simple llm inference acceleration framework with multiple decoding heads. *arXiv preprint arXiv:2401.10774*, 2024. 1

[5] Charlie Chen, Sebastian Borgeaud, Geoffrey Irving, Jean-Baptiste Lespiau, Laurent Sifre, and John Jumper. Accelerating large language model decoding with speculative sampling. *arXiv preprint arXiv:2302.01318*, 2023. 1, 2

[6] Wei-Lin Chiang, Zhuohan Li, Zi Lin, Ying Sheng, Zhanghao Wu, Hao Zhang, Lianmin Zheng, Siyuan Zhuang, Yonghao Zhuang, Joseph E. Gonzalez, Ion Stoica, and Eric P. Xing. Vicuna: An open-source chatbot impressing gpt-4 with 90%* chatgpt quality, 2023. 3

[7] Aakanksha Chowdhery, Sharan Narang, Jacob Devlin, Maarten Bosma, Gaurav Mishra, Adam Roberts, Paul Barham, Hyung Won Chung, Charles Sutton, Sebastian Gehrmann, et al. Palm: Scaling language modeling with pathways. *Journal of Machine Learning Research*, 24(240): 1–113, 2023. 1

[8] Cunxiao Du, Jing Jiang, Xu Yuanchen, Jiawei Wu, Sicheng Yu, Yongqi Li, Shenggui Li, Kai Xu, Liqiang Nie, Zhaopeng Tu, et al. Glide with a cape: A low-hassle method to accelerate speculative decoding. *arXiv preprint arXiv:2402.02082*, 2024. 1

[9] Yichao Fu, Peter Bailis, Ion Stoica, and Hao Zhang. Break the sequential dependency of llm inference using lookahead decoding. *arXiv preprint arXiv:2402.02057*, 2024. 1

[10] Mukul Gagrani, Raghavv Goel, Wonseok Jeon, Junyoung Park, Mingu Lee, and Christopher Lott. On speculative decoding for multimodal large language models. In *Proceedings of the IEEE/CVF Conference on Computer Vision and Pattern Recognition*, pages 8285–8289, 2024. 2, 6

[11] Yash Goyal, Tejas Khot, Douglas Summers-Stay, Dhruv Batra, and Devi Parikh. Making the v in vqa matter: Elevating the role of image understanding in visual question answering. In *Proceedings of the IEEE conference on computer vision and pattern recognition*, pages 6904–6913, 2017. 7

[12] Minjae Lee, Wonjun Kang, Byeongkeun Ahn, Christian Classen, Minghao Yan, Hyung Il Koo, and Kangwook Lee. In-batch ensemble drafting: Robust specula-tive decoding for lvlms. 2

[13] Yaniv Leviathan, Matan Kalman, and Yossi Matias. Fast inference from transformers via speculative decoding. In *International Conference on Machine Learning*, pages 19274–19286. PMLR, 2023. 1, 2

[14] Junnan Li, Dongxu Li, Silvio Savarese, and Steven Hoi. Blip-2: Bootstrapping language-image pre-training with frozen image encoders and large language models. In *International conference on machine learning*, pages 19730–19742. PMLR, 2023. 1

[15] Yuhui Li, Fangyun Wei, Chao Zhang, and Hongyang Zhang. Eagle: Speculative sampling requires rethinking feature uncertainty. *arXiv preprint arXiv:2401.15077*, 2024. 1, 6

[16] Yuhui Li, Fangyun Wei, Chao Zhang, and Hongyang Zhang. Eagle-2: Faster inference of language models with dynamic draft trees. *arXiv preprint arXiv:2406.16858*, 2024. 2, 3, 5, 7, 8

[17] Luxi Lin, Zhihang Lin, Zhanpeng Zeng, and Rongrong Ji. Speculative decoding reimagined for multimodal large language models. *arXiv preprint arXiv:2505.14260*, 2025. 2, 6, 7, 8

[18] Haotian Liu, Chunyuan Li, Qingyang Wu, and Yong Jae Lee. Visual instruction tuning, 2023. 1, 3, 7

[19] Haotian Liu, Chunyuan Li, Yuheng Li, Bo Li, Yuanhan Zhang, Sheng Shen, and Yong Jae Lee. Llava-next: Improved reasoning, ocr, and world knowledge, 2024. 1, 2, 7

[20] Pan Lu, Swaroop Mishra, Tanglin Xia, Liang Qiu, Kai-Wei Chang, Song-Chun Zhu, Oyvind Tafjord, Peter Clark, and Ashwin Kalyan. Learn to explain: Multimodal reasoning via thought chains for science question answering. *Advances in Neural Information Processing Systems*, 35:2507–2521, 2022. 7

[21] Ahmed Masry, Do Xuan Long, Jia Qing Tan, Shafiq Joty, and Enamul Hoque. Chartqa: A benchmark for question answering about charts with visual and logical reasoning. *arXiv preprint arXiv:2203.10244*, 2022. 7

[22] Amanpreet Singh, Vivek Natarajan, Meet Shah, Yu Jiang, Xinlei Chen, Dhruv Batra, Devi Parikh, and Marcus Rohrbach. Towards vqa models that can read. In *Proceedings of the IEEE/CVF conference on computer vision and pattern recognition*, pages 8317–8326, 2019. 7

[23] Hanshi Sun, Zhuoming Chen, Xinyu Yang, Yuandong Tian, and Beidi Chen. Triforce: Lossless acceleration of long sequence generation with hierarchical speculative decoding. *arXiv preprint arXiv:2404.11912*, 2024. 1

[24] Qwen Team. Qwen2 technical report. *arXiv preprint arXiv:2407.10671*, 2, 2024. 3

[25] Hugo Touvron, Thibaut Lavril, Gautier Izacard, Xavier Martinet, Marie-Anne Lachaux, Timothée Lacroix, Baptiste Rozière, Naman Goyal, Eric Hambro, Faisal Azhar, et al.

Llama: Open and efficient foundation language models. *arXiv preprint arXiv:2302.13971*, 2023. 1, 3

[26] Peng Wang, Shuai Bai, Sinan Tan, Shijie Wang, Zhihao Fan, Jinze Bai, Keqin Chen, Xuejing Liu, Jialin Wang, Wenbin Ge, et al. Qwen2-vl: Enhancing vision-language model's perception of the world at any resolution. *arXiv preprint arXiv:2409.12191*, 2024. 3

[27] Xinlong Wang, Xiaosong Zhang, Zhengxiong Luo, Quan Sun, Yufeng Cui, Jinsheng Wang, Fan Zhang, Yueze Wang, Zhen Li, Qiying Yu, et al. Emu3: Next-token prediction is all you need. *arXiv preprint arXiv:2409.18869*, 2024. 3

[28] Heming Xia, Tao Ge, Peiyi Wang, Si-Qing Chen, Furu Wei, and Zhifang Sui. Speculative decoding: Exploiting speculative execution for accelerating seq2seq generation. *arXiv preprint arXiv:2203.16487*, 2022. 1

[29] Wenda Xu, Rujun Han, Zifeng Wang, Long T Le, Dhruv Madeka, Lei Li, William Yang Wang, Rishabh Agarwal, Chen-Yu Lee, and Tomas Pfister. Speculative knowledge distillation: Bridging the teacher-student gap through interleaved sampling. *arXiv preprint arXiv:2410.11325*, 2024. 6

[30] Lefan Zhang, Xiaodan Wang, Yanhua Huang, and Ruiwen Xu. Learning harmonized representations for speculative sampling. *arXiv preprint arXiv:2408.15766*, 2024. 3, 6